The Journal of Immunology

Differences in the Kinetics, Amplitude, and Localization of ERK Activation in Anergy and Priming Revealed at the Level of Individual Primary T Cells by Laser Scanning Cytometry

Claire L. Adams, Angela M. Grierson, Allan M. Mowat, Margaret M. Harnett and Paul Garside

J Immunol 2004; 173:1579-1586; ;
doi: 10.4049/jimmunol.173.3.1579
http://www.jimmunol.org/content/173/3/1579

The Journal of Immunology is published twice each month by
The American Association of Immunologists, Inc.,
1451 Rockville Pike, Suite 650, Rockville, MD 20852

Print ISSN: 0022-1767 Online ISSN: 1550-6606.

Differences in the Kinetics, Amplitude, and Localization of ERK Activation in Anergy and Priming Revealed at the Level of Individual Primary T Cells by Laser Scanning Cytometry[1]

Claire L. Adams, Angela M. Grierson, Allan M. Mowat, Margaret M. Harnett, and Paul Garside[2]

One of the potential mechanisms of peripheral tolerance is the unresponsiveness of T cells to secondary antigenic stimulation as a result of the induction of anergy. It has been widely reported that antigenic unresponsiveness may be due to uncoupling of MAPK signal transduction pathways. However, such signaling defects in anergic T cell populations have been mainly identified using immortalized T cell lines or T cell clones, which do not truly represent primary Ag-specific T cells. We have therefore attempted to quantify signaling events in murine primary Ag-specific T cells on an individual cell basis, using laser-scanning cytometry. We show that there are marked differences in the amplitude and cellular localization of phosphorylated ERK p42/p44 (ERK1/2) signals when naive, primed and anergic T cells are challenged with peptide-pulsed dendritic cells. Primed T cells display more rapid kinetics of phosphorylation and activation of ERK than naive T cells, whereas anergic T cells display a reduced ability to activate ERK1/2 upon challenge. In addition, the low levels of pERK found in anergic T cells are distributed diffusely throughout the cell, whereas in primed T cells, pERK appears to be targeted to the same regions of the cell as the TCR. These data suggest that the different consequences of Ag recognition by T cells are associated with distinctive kinetics, amplitude, and localization of MAPK signaling. ***The Journal of Immunology*****, 2004, 173: 1579–1586.**

Peripheral tolerance is a state of Ag-specific hyporesponsiveness induced by exposure of T cells to Ag under suboptimal activating conditions (1). Once it is induced, it can suppress many aspects of the Ag-specific immune response to subsequent challenge, including lymphocyte proliferation, cytokine production, in vivo delayed-type hypersensitivity, and Ab production (2). However, the molecular mechanisms underlying this phenomenon remain unclear (3, 4).

T lymphocyte activation requires at least two signals generated from the APC: the first is specific recognition of peptide-MHC by the TCR (signal 1), and the second is costimulation provided by molecules such as CD80/CD86 on the APC interacting with CD28 on the T cell (signal 2) (5). It is well established that TCR ligation in the absence of costimulation induces long-lasting unresponsiveness (anergy) in T cells (6, 7). Several methods have been used to induce anergy in vitro (8–10), including exposure to immobilized anti-CD3 in the absence of costimulatory signals (11, 12). Under these conditions restimulation with immunogenic Ag leads to a profound decrease in IL-2 production and, hence, proliferation. In T cells, anergy reflects defective activation of transcription factors, such as c-Jun/c-Fos, that are involved in formation of the AP-1 complex, which is required for inducing transcription of the IL-2 gene (13–19). In turn, this appears to be determined by the differential recruitment of the signaling cascades mediated by ERK, JNK, and p38 MAPK (13, 15, 16).

To date, studies investigating the activation state of the various MAPK signaling cascades in anergy have been limited to T cell clones in vitro, essentially because of the limitations imposed by the large number of cells required for conventional biochemical methodology (20). However, these studies may not be representative of primary T cells. Indeed, the ability to track Ag-specific T cells (21–23) and signal transduction events in vivo has shown that conclusions based on in vitro studies may not reflect what occurs under physiological conditions (24). In this study we have addressed these issues by developing a laser-scanning cytometry (LSC)[3] method that can quantify signaling events in individual Ag-specific T cells within heterogeneous cell populations. Using this approach we have investigated whether activation patterns and cellular distribution of the ERK differed among anergized, naive, and primed primary T cells upon challenge with Ag loaded APC in vitro.

Materials and Methods

Mice

D011.10 TCR transgenic (Tg) mice on a BALB/c background were used (25). These Tg T cells recognize $OVA_{323–339}$ and are detectable using the KJ1-26 clonotypic Ab (26). All animals were specified pathogen free and were maintained under standard animal house conditions in accordance with Home Office regulations.

Induction and assessment of anergy and priming in T cells

Peripheral (axillary, inguinal, and cervical) and mesenteric lymph nodes were removed from D011.10 transgenic mice, and T cells were purified using T cell enrichment immunocolumns (Cellect; V_H Bio, Gateshead, U.K.). Purified T cell suspensions (75–85% $CD4^+KJ1\text{-}26^+$ T cells as assessed by flow cytometry (23)) were cultured in complete medium at a concentration of 1×10^6 cells/ml/well (RPMI 1640, 10% FCS, 2 mM

Division of Immunology, Infection and Inflammation, University of Glasgow, Western Infirmary, Glasgow, United Kingdom

Received for publication April 5, 2004. Accepted for publication May 19, 2004.

The costs of publication of this article were defrayed in part by the payment of page charges. This article must therefore be hereby marked *advertisement* in accordance with 18 U.S.C. Section 1734 solely to indicate this fact.

[1] This work was supported by a Medical Research Council grant (to P.G., M.M.H., and A.M.).

[2] Address correspondence and reprint requests to Dr. Paul Garside, Division of Immunology, Infection and Inflammation, University of Glasgow, Western Infirmary, Glasgow, U.K. G11 6NT. E-mail: paul.garside@clinmed.gla.ac.uk

[3] Abbreviations used in this paper: LSC, laser-scanning cytometry; DAPI, 4′,6-diamido-2-phenylindole hydrochloride; DC, dendritic cell; Tg, transgenic.

0022-1767/04/$02.00

L-glutamine, 100 U/ml penicillin, 100 U/ml streptomycin, and 0.05 mM 2-ME; all from Invitrogen Life Technologies, Paisley, U.K.) with 1 μg/ml immobilized anti-CD3 (clone 145-2C11) for 48 h in the presence or the absence of 1 μg/ml anti-CD28 (clone 37.51; BD Pharmingen, Oxford, U.K.). After 48 h, cells were washed twice with RPMI 1640, replated, and rested in complete medium for an additional 48 h (11, 12). The viable Tg T cells were then counted by trypan blue exclusion and restimulated by culture with LPS-matured (see below), peptide ($OVA_{323–339}$)-loaded dendritic cells (DC) at a ratio of 1:1 (10^5 T cells and 10^5 DC in 400 μl of medium/chamber) in four-well chamber slides (SLS, Nottingham, U.K.). The DC were bone marrow derived (27) and grown in DC medium (5% GM-CSF, RPMI 1640, 10% FCS, 2 mM L-glutamine, 100 U/ml penicillin, 100 U/ml streptomycin, and 0.05 mM 2-ME) for 9 days before maturation with 1 μg/ml LPS (*Salmonella abortus*; Sigma-Aldrich, Poole, U.K.) for 24 h. OVA peptide 323–339 (1 μg/ml; Genosys; Sigma-Aldrich) was added to the matured DC for 3–4 h, which were then washed extensively before use.

After restimulation, the cells were fixed in PBS containing 1% paraformaldehyde before staining. To study cell cycle progression and cellular localization of ERK, cytospins were prepared by cytocentrifuging cells onto microscope slides at 600 rpm for 4 min using a Cytospin 3 centrifuge (Thermo Shandon, Runcorn, U.K.), then fixed in 4% formaldehyde in PBS for 15 min on ice.

Flow cytometry

Aliquots of cells (10^6/ml) were incubated with FcR blocking buffer (anti-CD16/32, clone 4.G-2, hybridoma supernatant, 10% mouse serum, and 0.1% sodium azide) for 10 min at 4°C. Cells were then incubated with CD4-PerCP, CD69-PE, and biotinylated anti-TCR Ab, KJ1-26, for 40 min at 4°C; washed in FACS buffer (PBS, 2% FCS, and 0.05% sodium azide); and then incubated with FITC-conjugated streptavidin (Vector Laboratories, Burlingame, CA) for 30 min at 4°C. Cells were washed again in FACS buffer and resuspended in FACS flow for analysis with a FACScan and CellQuest software (BD Pharmingen). Three-color analysis was performed on 20,000 events.

Proliferation assays and cytokine production

Anergized (anti-CD3 only), activated (anti-CD3 and anti-CD28), and naive (freshly isolated) primary T cells (10^5 cells/well) were cultured with LPS-matured, peptide-loaded DC for 48 h, pulsed with 1 μCi/well [^{3}H]thymidine (Western Infirmary, Glasgow, U.K.), and harvested after an additional 16 h. Where indicated, 10 ng/ml rIL-2 (gift from Dr. D. Xu, Western Infirmary) was added at the beginning of the proliferation assay. The amount of IL-2 in culture supernatants was measured, after 20-h restimulation, by ELISA using a rat anti-mouse IL-2 capture Ab, biotinylated rat anti-mouse detection Ab (BD Pharmingen), and streptavidin peroxidase (Sigma-Aldrich). The ELISA standard curve was generated using recombinant murine IL-2 as a standard (R&D Systems, Minneapolis, MN).

Western blotting

Anergized, activated, and naive T cells (10^6) were harvested and lysed in lysis buffer (50 mM Tris-HCl (pH 7.5), 150 mM NaCl, 2% (v/v) Nonidet P-40, 0.25% (w/v) sodium deoxycholate, 1 mM EDTA (pH 8.0), 1 mM PMSF, 10 mM sodium orthovanadate, 10 μg/ml chymostatin, 10 μg/ml leupeptin, 10 μg/ml antipain, and 10 μg/ml pepstatin A; Sigma-Aldrich) for 20 min on ice. The cellular debris was removed by centrifugation at 12,000 rpm for 10 min at 4°C, and the protein concentration of the soluble fraction was determined using the Micro BCA protein assay reagent kit (Pierce, Rockford, IL). Samples (75 μg) were mixed with an equal volume of 2× SDS-PAGE gel loading buffer (20% (v/v) glycerol, 4% (w/v) SDS, 100 mM Tris-HCl (pH 6.8), 2 μg/ml bromophenol blue, and 5% (w/v) 2-ME), boiled, and separated on 10% SDS-PAGE gel (Bio-Rad, Hercules, CA). Proteins were then transferred onto nitrocellulose membranes (Amersham International, Little Chalfont, U.K.), and nonspecific binding sites were blocked with TBS (2 M NaCl, 20 mM Tris-HCl (pH 7.5), and 0.1% Tween 20) containing 5% nonfat dry milk. Immunodetection was accomplished by incubating the membranes first with primary Abs that recognize total or active ERK1 and ERK2 (either rabbit anti-p44/42 MAPK or rabbit anti-dually phosphorylated p44/42 MAPK; Cell Signaling Technology, New England Biolabs, Beverly, MA) and then with an anti-rabbit IgG HRP-conjugated secondary Ab (1/2000; Cell Signaling Technology) diluted in TBS/5% nonfat dry milk. The immunocomplexes were detected using chemiluminescence (ECL, Amersham International).

Intracellular staining of cells

Cells were attached to microscope slides or cultured in chamber slides, fixed, washed in PBS, and placed in 1% blocking reagent (Molecular Probes, Eugene, OR) for 30 min. All Abs were diluted in 1% blocking reagent, and washing steps were conducted three times in TNT buffer (0.15 M NaCl, 0.1 M Tris-HCl (pH 7.5), and 0.05% Tween 20) unless otherwise stated.

Cells were incubated with biotinylated anti-KJ1.26 for 30 min, washed, and then incubated with streptavidin-HRP for 30 min. After washing, the cells were treated with biotinylated-tyramide (TSA biotin system; PerkinElmer Life Sciences, Boston, MA) for 10 min, washed, and then incubated with streptavidin-Alexa Fluor 647 (all Alexa Fluor dyes were purchased from Molecular Probes) for 30 min. Excess HRP was quenched using 0.1% sodium azide/3% hydrogen peroxide in PBS for 10 min, and this quenching step was repeated three times.

Cells were permeabilized for 5 min in permeabilization buffer (2% FCS, 2 mM EDTA (pH 8.0), and 0.1% saponin) and incubated for 15 min in 1% blocking reagent. Saponin (final concentration, 0.1%) was added to all Ab staining stages when detecting intracellular proteins. Cells were incubated with anti-phospho-p44/42 or anti-p44/42 MAPK for 30 min, washed, and then treated with anti-rabbit IgG HRP conjugate (Molecular Probes). Finally, Alexa Fluor 488 tyramide was added for 10 min, washed, and mounted in Vectashield with 4′,6-diamido-2-phenylindole hydrochloride (DAPI; Vector Laboratories). Biotinylated rat anti-mouse IgG2a (BD Pharmingen) and rabbit anti-Ig (Sigma-Aldrich) served as isotype-negative controls for biotinylated KJ1-26 and p44/42 MAPK, respectively.

Immunofluorescence microscopy and LSC

Fluorescence of individual cells was measured using LSC (Compucyte, Cambridge, MA). Briefly, Alexa Fluor-488 (absorbance, 495 nm; emission, 519 nm) was excited using the argon ion laser and was measured using filter cube D 530/30 nm. Alexa Fluor-647 (absorbance, 650 nm; emission, 665 nm) was excited using the He-Ne laser and was measured using filter cube H1 650/LPCy5 nm. DAPI (absorbance, 359 nm; emission, 461 nm) was excited using the UV laser. Photomultiplier tube values were adjusted at the start of each batch of experiments to optimize fluorescence excitation (28, 29).

When analyzing chamber slides/cytospins, the primary contouring parameter was set on the nuclear localization of the DNA dye, DAPI, to detect all of the cellular events within the population. Detector gain voltages (photomultiplier tubes) were set at the maximum of 75% saturation for optimizing the pixel event for each fluorophore. Using the LSC scan data display, the threshold contour was placed around the nucleus, and the integration contour was located 11 pixels (1 pixel = 0.5 μm (*x*-axis) × 0.25 μm (*y*-axis) for ×40 objective) outside the threshold contour, which approximately defined the edge of the cell. This integration contour allowed us to calculate the total fluorescence within each cell (fluorescence integral value). Additionally, peripheral contours were set to measure fluorescence within various regions of the cell, specified using inner and outer boundaries 12 pixels wide. Background fluorescence was measured outside the cell and automatically subtracted from the measured fluorescence values. For analysis purposes the positive gate was positioned according to the fluorescence obtained using appropriate negative/isotype controls. LSC data analysis was conducted using Wincyte version 3.6 (Compucyte).

Fluorescence images were taken using a connected 3CCD color vision camera (regulated by a Hamamatsu and Orbit controller) and the Openlab version 3.0.9 digital imaging program (Improvision, Warwick, U.K.).

Results

Induction of anergy and priming in primary T cells

T cell anergy was induced in primary OVA-specific D011.10 T cells by TCR engagement without appropriate costimulation as described previously (11, 12). The T cells were cultured for 48 h on plate-bound anti-CD3 with or without costimulation via anti-CD28. These cells were then washed and rested for an additional 2 days in fresh medium before being restimulated with LPS-matured DC with or without OVA peptide $_{323–339}$ (Fig. 1*A*).

Freshly isolated D011.10 T cells (naive T cells) proliferated well in response to challenge with peptide-loaded DC, and this response was significantly higher when T cells precultured with anti-CD3 and anti-CD28 (primed T cells) were used (Fig. 1*B*). These responses were significantly lower when T cells precultured with anti-CD3 were used (anergic T cells), confirming the induction of

anergy. This decrease in proliferation was partly rescued by the addition of exogenous rIL-2, as it increased the proliferation of anergic T cells to levels equal to or greater than those reached by primed or naive T cells stimulated with Ag in the absence of exogenous rIL-2.

As expected, restimulated anergic T cells also showed a defect in IL-2 production upon restimulation compared with that found with naive and primed D011.10 T cell populations (Fig. 1*C*). Importantly, the defects in IL-2 production and proliferation were not due to the failure of the anergic T cells to recognize Ag after restimulation, because they increased expression of the early activation marker CD69 to the same extent as primed T cells (Fig. 1*D*). Together, these findings indicate that the different in vitro primary culture regimens induce T cell priming or anergy.

Cell cycle progression after restimulation with Ag

Ag-specific unresponsiveness at the level of individual T cells can involve either apoptotic cell death or anergy, in which cells survive, but show cell cycle arrest at the G_1-S transition (30). To assess these mechanisms quantitatively, we investigated cell cycle progression in the different T cell populations using LSC (31–33) (Fig. 2*A*). Moreover, the application of this technology allowed us to examine whether differences in ERK-MAPK signaling were associated with cell cycle progression in the different T cell populations, as suggested previously (34–37). Therefore, we analyzed the activation status of ERK-MAPK at each stage of the cell cycle.

As productive stimulation has been reported to induce naive primary T cells to enter the cell cycle within 12 h (35), cell populations were analyzed 20 h after challenge with Ag to assess S phase transition. An example of this kind of analysis is shown in Fig. 2*A*, which demonstrates the ability of the LSC to detect all stages of the cell cycle. As expected, the primed T cell population displayed a greater percentage of mitotic and newly formed daughter cells compared with either naive or tolerized T cells, whereas progression into S phase within the anergic population was reduced compared with the naive and primed groups (Fig. 2*B*). In addition, a substantial proportion of anergic T cells were apoptotic, as shown by LSC (Fig. 2*B*) and TUNEL (data not shown). Apoptotic cells were relatively rare in the

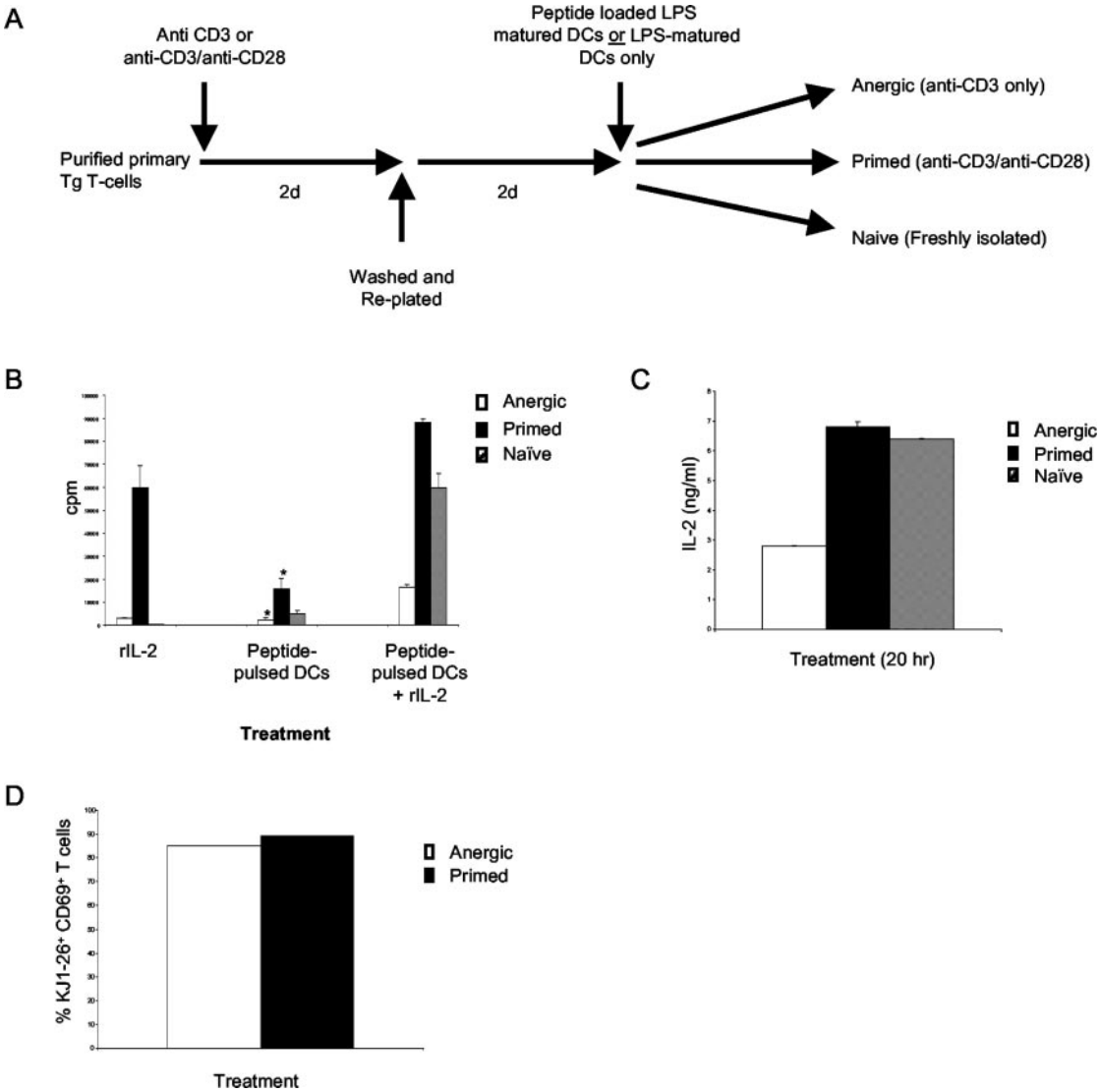

FIGURE 1. Induction of anergy in Ag-specific TCR Tg T cells. Anergic and primed T cells were generated using immobilized anti-CD3 and soluble anti-CD28 in vitro as indicated (*A*). Naive T cells were freshly isolated (*A*). Levels of proliferation (*B*) and IL-2 production (*C*), measured at 48 and 20 h, respectively, were lower in anergic (□) compared with the primed (■) and naive (▨) T cell populations, after restimulation with $OVA_{323–339}$-pulsed DC. Surface expression of the early T cell activation marker, CD69, was similar in both anergic and primed T cells throughout the experiment (*D*). The results shown are the mean ± 1 SD of triplicate cultures and are representative of five individual experiments. ∗, $p \leq 0.05$.

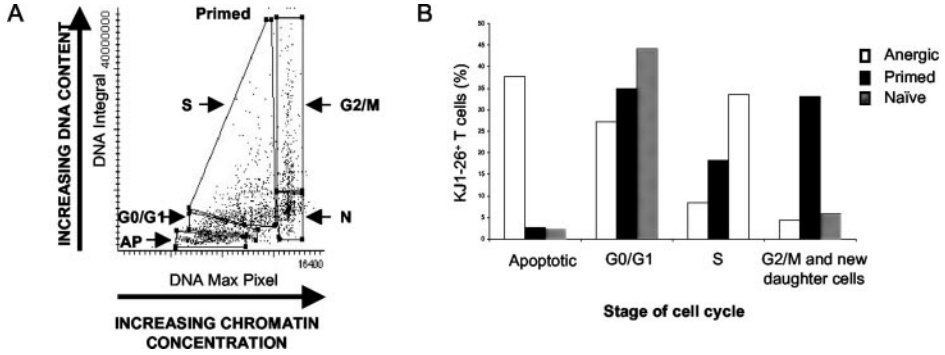

FIGURE 2. Analysis of cell cycle progression of Ag-specific primary T cells after stimulation with Ag-pulsed APCs by LSC. Primed cells were restimulated with LPS-matured DC loaded with $OVA_{323–339}$ or DC alone for 20 h, and the cell cycle status of 1000 transgenic KJ1.26$^+$ T cells was analyzed after staining with DAPI. The maximum pixel value (depicting chromatin condensation) is plotted along the *x*-axis, and the integral value (representing DNA content) is shown along the *y*-axis. Apoptotic (AP) cells are characterized by low (sub G_1) DNA content (*A*), and the percentage of T cells within the different stages of the cell cycle was determined. Data are representative of four identical experiments.

primed or naive populations. By using the LSC to assess the amount of pERK in individual T cells within the various regions of the cell cycle plot, we were also able to show that an increase in pERK expression correlates with cell cycle progression upon activation of primed T cells with higher levels in G_2/M and S phase and new daughter cells (Table I).

Anergic T cells display reduced activation of ERK-MAPK

Previous studies have identified uncoupling of the ERK-MAPK pathway as a key mechanism that leads to Ag-specific unresponsiveness in anergic T cells (13–18). However, most these studies have been conducted using T cell clones and hence may not be representative of the situation in normal T cells. Therefore, we used LSC to assess the expression of pERK in individual anergic Ag-specific CD4$^+$ T cells and validated the results by conventional biochemical means of assessing T cell signaling.

Standard Western blotting techniques showed that the amount of pERK1/2 was higher in all groups of T cells restimulated with peptide-loaded DC compared with unpulsed DC (Fig. 3). However, the levels of activated ERK were reproducibly lower in anergic T cells than in either the primed or naive T cell populations.

To establish whether LSC was capable of detecting these differences in the activation of ERK in primary T cells at the single-cell level, we developed a method to analyze the phosphorylation state of signaling molecules using chamber slides and three-color immunofluorescence, initially comparing the amount of ERK phosphorylation in primed T cells in the presence or the absence of Ag. Cells were identified by nuclear staining with the DNA dye DAPI (Fig. 4*A*). Those cells (mixture of APC and T cells) positive for the transgenic TCR were then identified by staining with the clonotypic Ab (KJ1-26; Fig. 4*B*), and the expression of activated ERK within these cells was determined with an Ab specific for pERK (Fig. 4*C*). Merging of these images (Fig. 4*D*) allowed assessment of pERK in Ag-specific T cells. This showed that all the KJ1-26$^+$ T cells restimulated with Ag-loaded APC were also pERK$^+$, whereas KJ1-26$^+$ T cells exposed to APC alone showed little or no pERK staining (Fig. 4, *D* vs *E*). When anergized T cells were examined (Fig. 4*F*), a far lower proportion of TCR Tg T cells expressed pERK upon restimulation, and those few cells that did express pERK appeared to do so at a lower level (Fig. 4, *D* vs *F*). LSC was then used to quantify these apparent differences in pERK expression. In agreement with the Western blot analysis, ERK activation was elevated in all samples challenged with Ag (Fig. 5*A*), although the phosphorylation of ERK in primed T cells was more rapid than in the naive T cell population, peaking at 30 min in the former and at 60 min in the latter (data not shown). Although the analysis shown demonstrates similar levels of pERK in naive and primed T cells, kinetic studies revealed that this was always lower in the anergic population than in either naive or primed T cells. However, further analysis revealed that not only was the overall level of pERK lower in the anergic T cell population (Fig. 5*A*), but the proportion of Ag-stimulated cells expressing pERK in this group was lower than in all other groups (Fig. 5*B*). Moreover, those anergized T cells that expressed pERK did so at a lower level than the other groups (Fig. 5*C*).

Table I. *pERK expression in cell cycle progression*

Stage of Cell Cycle	% Primed KJ1–26$^+$ T Cells in That Stage	% Primed KJ1–26$^+$ T Cells in That Stage Expressing pERK
G_0/G_1	2.8	64.3
S phase (S)	23	86.3
G_2/M	27.5	90.4
New daughter cells (N)	31	86.1

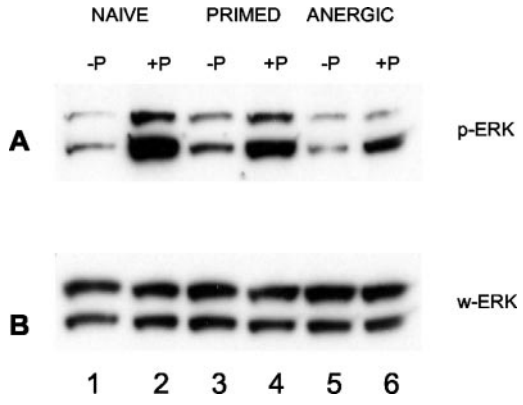

FIGURE 3. Anergic cells exhibit reduced levels of pERK relative to primed cells after restimulation. Activation levels of ERK1/2 1 h after rechallenge with LPS-matured DC loaded with $OVA_{323–339}$ or DC alone were measured using Western blot analysis of pERK1/2 (*A*) and total ERK1/2 (*B*) levels in whole cell lysates. *Lane 1*, Naive T cells and APC; *lane 2*, naive T cells and Ag/APC; *lane 3*, primed T cells and APC; *lane 4*, primed T cells and Ag/APC; *lane 5*, anergized T cells and APC; *lane 6*, anergized T cells and Ag/APC. The data are representative of at least three independent experiments.

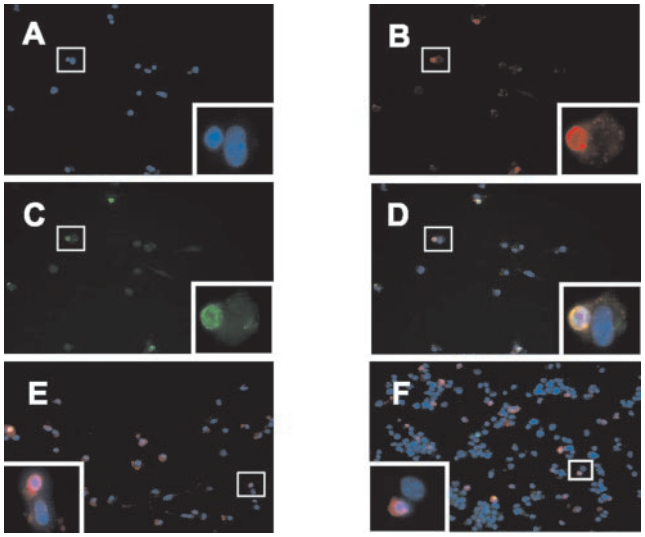

FIGURE 4. Visualization of ERK activation using three-color immunofluorescence. Cells were identified by nuclear staining with the DNA dye DAPI (*A*, blue) and for the transgenic TCR by staining with the clonotypic Ab (KJ1-26; *B*, red). The expression of activated ERK was then determined with an Ab specific for pERK (*C*, green). Merging these images (*D*) allowed assessment of pERK in Ag-specific T cells in the presence (*D*) or the absence (*E*) of Ag. Primed (*A–E*) and anergized (*F*) T cells are represented. Fields of view were taken at ×20 magnification, with the *inset* representing a single T cell-APC interaction (depicted by the square; ×40 magnification).

Intracellular localization of pERK expression

LSC also has the capacity to quantify fluorescence changes within intracellular compartments within an individual cell, thus permitting localization of signaling molecules within T cells. The pERK appeared to be localized mainly at the periphery of primed T cells stimulated with Ag, whereas it was distributed more diffusely throughout the cell in those anergized T cells that expressed low levels of pERK (Fig. 6, *A* and *B*, *i–iii*). When the levels of pERK in the periphery of cells were quantified using the gating and peripheral contouring facilities on the LSC, 1 h after challenge with Ag, primed T cells contained more pERK than anergic T cells (Fig. 6*C*). Furthermore, the primed T cells displayed an accumulation of pERK in the periphery of the cells, which was not apparent in anergic T cells (Fig. 6*Cii*).

Discussion

It has been widely proposed that both qualitative and quantitative differences in T cell signaling may underlie the differential functional outcomes of immunological tolerance and priming (38, 39). However, much of the work to date has relied upon biochemical assessment of signaling in T cell lines or clones at the population level following polyclonal stimulation in vitro, and this has yielded conflicting results. In this study, for the first time, we have compared the signaling events underlying Ag-specific responses in individual primary T cells and have demonstrated marked differences in the kinetics, amplitude, and localization of the MAPK-pERK pathway in priming and anergy.

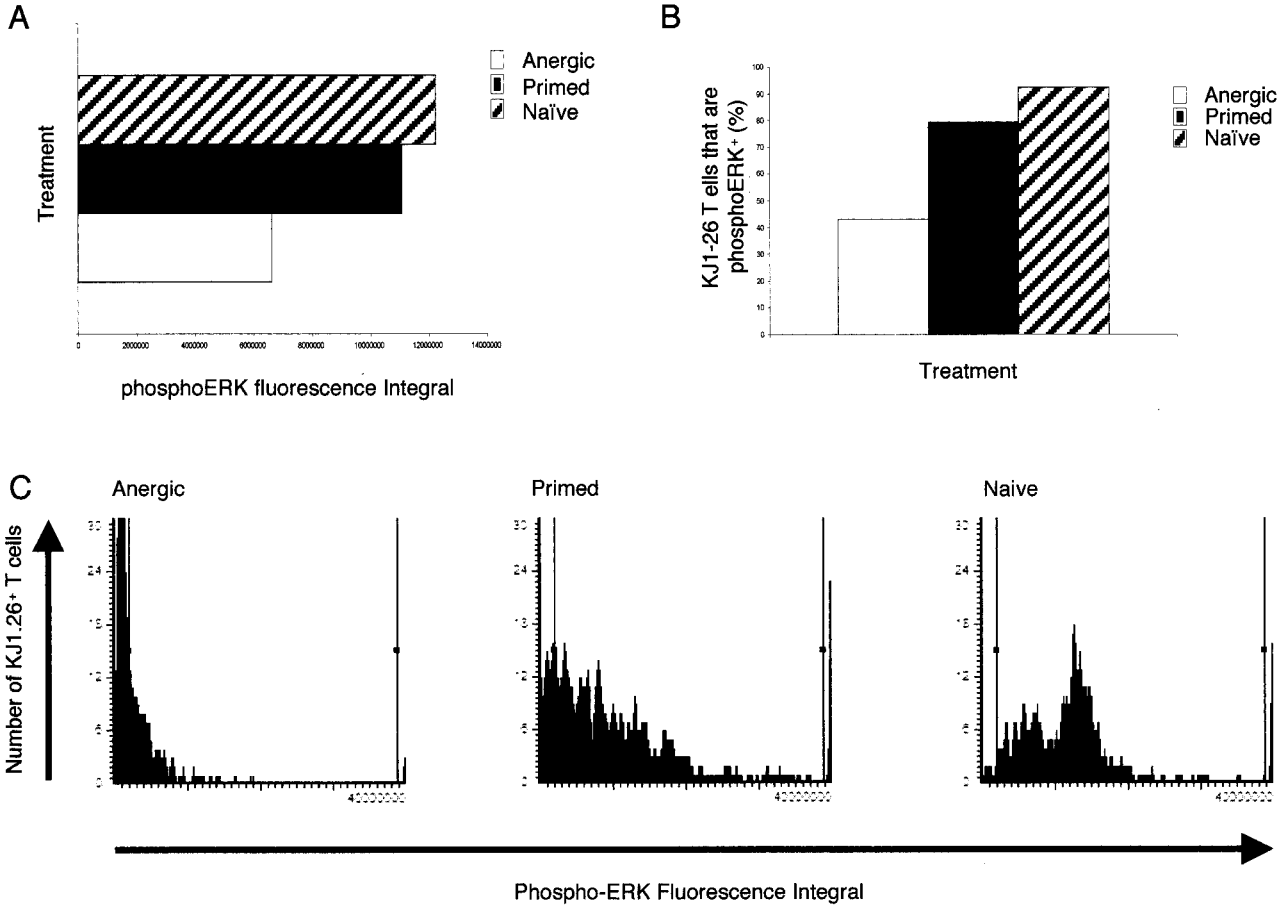

FIGURE 5. Quantitation of Ag-specific ERK activation by LSC. Total cellular expression of pERK at 20 h after Ag restimulation of naive, anergized, and primed KJ1-26$^+$ T cells is represented using the fluorescence integral value (*A*). The proportion of Ag-specific KJ1-26$^+$ T cells expressing pERK was also determined (*B*). The results shown are the average of 250 KJ1.26$^+$ transgenic T cells; the level of pERK expression within the TCR Tg T cells is also shown (*C*). Similar results were obtained in four replicate experiments.

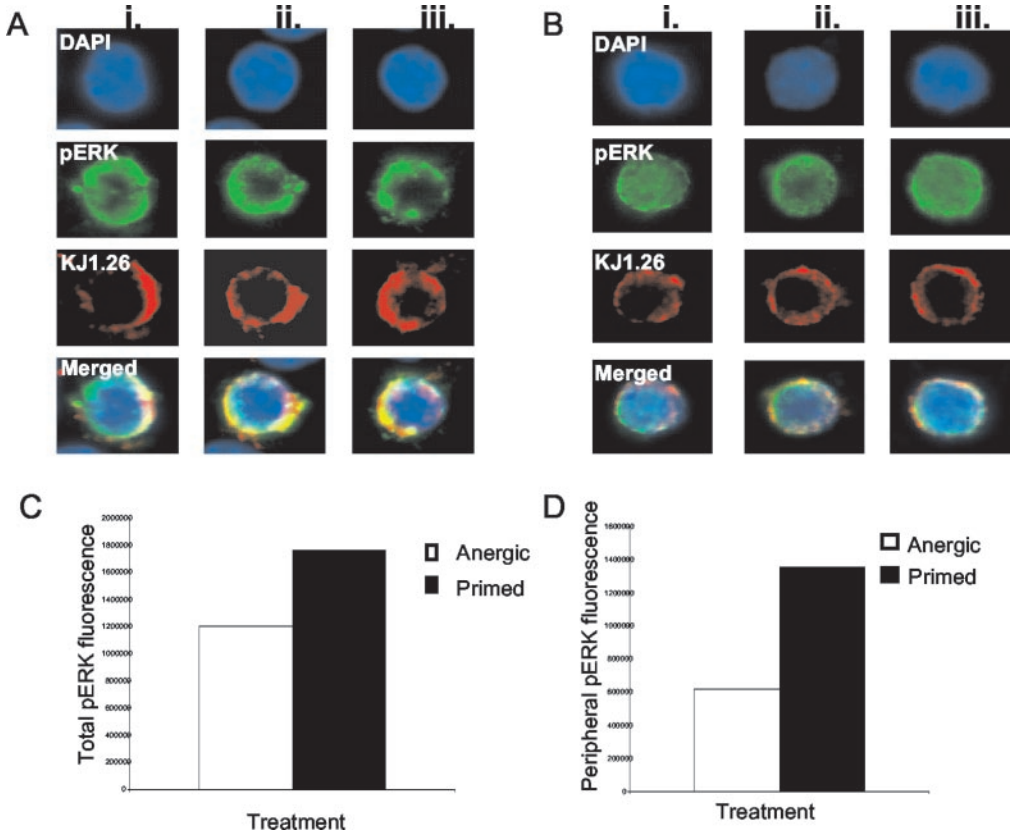

FIGURE 6. Intracellular localization of pERK staining in Ag-specific T cells. KJ1-26$^+$ pERK$^+$ T cells from primed and anergized populations were randomly relocated by LSC. Three representative individual primed or anergized T cells (*A* and *B*, *i–iii*) were identified by nuclear staining with the DNA dye DAPI (*A* and *B*, blue). Cells positive for Tg TCR were identified by staining with the clonotypic Ab (KJ1-26; *A* and *B*, red). The expression of activated ERK was determined with an Ab specific for pERK (*A* and *B*, green). Merging these images (*A* and *B*) allows assessment of the localization pERK in Ag-specific T cells in the presence of Ag. Turquoise represents a diffuse location of pERK (DAPI, blue; pERK, green), whereas yellow depicts a more peripheral cytoplasmic expression (KJ1-26, red; pERK, green; *C* and *D*). Diffuse vs peripheral localization of pERK was quantitated by peripheral contouring with LSC (*C*). Total (*C*) and peripheral (*D*) pERK were quantified for 250 pERK$^+$ anergic T cells (□) and primed T cells (■).

T cells that have been tolerized or primed in vitro display different functional processes as a result of the signaling events that occur during the initial and subsequent encounters with Ag. Upon secondary challenge with Ag, productively primed T cells show a characteristic pattern of signaling events in vitro that are necessary for the transcription of the IL-2 gene and subsequent clonal expansion of these T cells. In contrast, anergized T cell lines/clones display defective proliferation and an inability to produce IL-2 upon challenge (40, 41). We have confirmed and extended these earlier findings by showing a decrease in Ag-specific proliferation and IL-2 production in primary Ag-specific T cells that had been tolerized by preculture with anti-CD3 in the absence of costimulation. In contrast, restimulated anergized T cells produced identical levels of IFN-γ (data not shown) and up-regulated CD69 to the same extent as T cells that had been primed with anti-CD3 and anti-CD28. These results confirm previous reports (30) and show that that the defects in proliferation and IL-2 production were not the result of a failure of Ag recognition by anergized T cells. In contrast to other in vitro work (30), the secondary response of our anergized T cells was only partly restored by exogenous IL-2, although it was restored to levels similar to those in primed cells responding to Ag. However, similar findings have been reported by others (38, 39, 42), and it seems that different forms of anergy may show differential sensitivity to IL-2-mediated reversal of tolerance. These include clonal anergy due to lack of CD28 costimulation and cell cycle arrest anergy induced by CTLA-4 signaling. Moreover, there is evidence for induction of multiple forms of anergy (43) resulting from lack of CD28 costimulation, in which the progression to S phase is mediated via both IL-2-dependent and -independent pathways (44, 45).

Although the precise molecular mechanisms underlying the induction and maintenance of anergy in vitro have not been defined, it has been associated with defective coupling of the TCR to early signaling events, such as the activation of ZAP-70, ERK, and JNK (38, 39). In addition, there may be up-regulation of inhibitory factors, such as the GTPase, Rap-1 (which may act to disrupt the Ras-ERK-MAPK pathway), and the cell cycle (cyclin-dependent kinase) inhibitor, p27^{kip1}. Interestingly, up-regulation of p27^{kip1} is associated with both IL-2-dependent and -independent forms of anergy (42). In all cases, these mechanisms appear to lead to G_1-S cell cycle arrest and increased apoptosis in anergized cells.

Previous studies have identified a role for ERK-MAPK in regulating cell cycle arrest within anergic cells, and this may reflect its ability to down-regulate p27^{kip1} (34–36, 46, 47). Moreover, we have recently shown that periodic cycling ERK activation is associated with the progression of lymphocytes through all stages of the cell cycle and that inhibition of this sustained, but cycling, ERK activation resulted in apoptosis (37). Consistent with this, our present studies, using both conventional biochemical techniques and quantitative single-cell analysis by LSC, show that although ERK activation was elevated in all populations of T cells challenged with Ag, it was always lower in the anergic population. Analysis at the single-cell level revealed that the proportion of

Ag-stimulated cells expressing pERK was also lower in the anergic relative to the primed groups, and the few anergized T cells that expressed pERK did so at a lower level than primed cells. These findings were consistent with the fact that primed, but not anergic, Ag-specific T cells progressed through the cell cycle and that such progression correlated with increasing levels of pERK. In contrast, the anergic T cells displayed a greater propensity to apoptose upon challenge.

Quantitation by LSC showed that the majority of the pERK signal appeared to be localized at the periphery of restimulated primed T cells, possibly in association with TCR. In contrast, pERK was distributed more diffusely throughout those anergized T cells that expressed lower levels of pERK. These results were somewhat surprising, because we had hypothesized that restimulation of primed cells would induce pERK to translocate to the nucleus to activate the transcription factors (48) required for IL-2 induction and believed that this process might be defective in anergic T cells. Rather, it appears that after priming, pERK may associate with cytoskeletal- and/or membrane-associated scaffolds, such as lipid rafts, containing TCR and other components of the proximal signaling cascade. Thus, these structures, or the association of pERK with them, may be defective in anergized T cells. In this respect there is increasing evidence that the cytoskeleton plays important roles, not only in organization of the immunological synapse (49), but also in signal transduction (50) by its ability to recruit signaling elements to adapter molecules in the synapse. Actin scaffolds have also been postulated to promote TCR signaling by preventing degradation of signaling elements (38, 51) and by directing lipid raft trafficking to the synapse (38). Although the precise molecular details are not clear, the recent finding that ERK-MAPK is an intermediate signal in the Vav/Rac2-mediated pathway (52), leading to nucleation of actin filaments and cytoskeleton remodeling at the immunological synapse (53), may provide a molecular rationale for our results.

References

1. Mowat, A. M. 2003. Anatomical basis of tolerance and immunity to intestinal antigens. *Nat. Rev. Immunol. 3:331*.
2. Garside, P., and A. M. Mowat. 2001. Oral tolerance. *Semin. Immunol. 13:177*.
3. Macian, F., F. Garcia-Cozar, S. H. Im, H. F. Horton, M. C. Byrne, and A. Rao. 2002. Transcriptional mechanisms underlying lymphocyte tolerance. *Cell 109:719*.
4. Sebille, F., B. Vanhove, and J. P. Soulillou. 2001. Mechanisms of tolerance induction: blockade of co-stimulation. *Philos. Trans. R. Soc. London B 356:649*.
5. Harding, F. A., J. G. McArthur, J. A. Gross, D. H. Raulet, and J. P. Allison. 1992. CD28-mediated signalling co-stimulates murine T cells and prevents induction of anergy in T-cell clones. *Nature 356:607*.
6. Alegre, M. L., K. A. Frauwirth, and C. B. Thompson. 2001. T-cell regulation by CD28 and CTLA-4. *Nat. Rev. Immunol. 1:220*.
7. Lechler, R., C. J-G, F. Marelli-Berg, and G. Lombardi. 2001. T-cell anergy and peripheral T-cell tolerance. *Philos. Trans. R. Soc. London B 356:625*.
8. Jenkins, M. K., and R. H. Schwartz. 1987. Antigen presentation by chemically modified splenocytes induces antigen-specific T cell unresponsiveness in vitro and in vivo. *J. Exp. Med. 165:302*.
9. Quill, H., and R. H. Schwartz. 1987. Stimulation of normal inducer T cell clones with antigen presented by purified Ia molecules in planar lipid membranes: specific induction of a long-lived state of proliferative nonresponsiveness. *J. Immunol. 138:3704*.
10. Boussiotis, V. A., G. J. Freeman, A. Berezovskaya, D. L. Barber, and L. M. Nadler. 1997. Maintenance of human T cell anergy: blocking of IL-2 gene transcription by activated Rap1. *Science 278:124*.
11. Chai, J.-G., and R. Lechler. 1997. Immobilized anti-CD3 mAb induces anergy in murine naive and memory $CD4^+$ T-cells in vitro. *Int. Immunol. 9:935*.
12. Jenkins, M., C. Chen, G. Jung, D. Mueller, and R. Schwartz. 1990. Inhibition of antigen-specific proliferation of type-1 murine T cell clones after stimulation with immobilized anti-CD3 monoclonal antibody. *J. Immunol. 144:16*.
13. DeSilva, D. R., W. S. Feeser, E. J. Tancula, and P. A. Scherle. 1996. Anergic T cells are defective in both jun NH_2-terminal kinase and mitogen-activated protein kinase signaling pathways. *J. Exp. Med. 183:2017*.
14. Kang, S. M., B. Beverly, A. C. Tran, K. Brorson, R. H. Schwartz, and M. J. Lenardo. 1992. Transactivation by AP-1 is a molecular target of T cell clonal anergy. *Science 257:1134*.
15. Fields, P. E., T. F. Gajewski, and F. W. Fitch. 1996. Blocked Ras activation in anergic $CD4^+$ T cells. *Science 271:1276*.
16. Li, W., C. D. Whaley, A. Mondino, and D. L. Mueller. 1996. Blocked signal transduction to the ERK and JNK protein kinases in anergic $CD4^+$ T cells. *Science 271:1272*.
17. Li, W., C. Whaley, J. Bonnevier, A. Mondino, M. Martin, K. Aagaard-Tillery, and D. Mueller. 2001. CD28 signaling augments Elk-1 dependent transcription at the c-*fos* gene during antigen-stimulation. *J. Immunol. 167:827*.
18. Mondino, A., C. D. Whaley, D. R. DeSilva, W. Li, M. K. Jenkins, and D. L. Mueller. 1996. Defective transcription of the IL-2 gene is associated with impaired expression of c-Fos, FosB, and JunB in anergic T helper 1 cells. *J. Immunol. 157:2048*.
19. Sundstedt, A., and M. Dohlsten. 1998. In vivo anergized $CD4^+$ T cells have defective expression and function of the activating protein-1 transcription factor. *J. Immunol. 161:5930*.
20. Asai, K., S. Hachimura, M. Kimura, T. Toraya, M. Yamashita, T. Nakayama, and S. Kaminogawa. 2002. T Cell hyporesponsiveness induced by oral administration of ovalbumin is associated with impaired NFAT nuclear translocation and $p27^{kip1}$ degradation. *J. Immunol. 169:4723*.
21. Kearney, E., K. Pape, D. Loh, and M. Jenkins. 1994. Visualization of peptide-specific T cell immunity and peripheral tolerance induction in vivo. *Immunity 1:327*.
22. Pape, K., E. Kearney, A. Khoruts, A. Mondino, R. Merica, Z. Chen, E. Ingulli, J. White, J. Johnson, and M. Jenkins. 1997. Use of adoptive transfer of T-cell-antigen-receptor-transgenic T cell for the study of T-cell activation in vivo. *Immunol. Rev. 156:67*.
23. Garside, P., E. Ingulli, R. R. Merica, J. G. Johnson, R. J. Noelle, and M. K. Jenkins. 1998. Visualisation of specific B and T lymphocyte interactions in the lymph node. *Science 281:96*.
24. Zell, T., A. Khoruts, E. Ingulli, J. Bonnevier, D. Mueller, and M. Jenkins. 2001. single cell analysis of signal transduction in CD4 T cells stimulated by antigen in vivo. *Proc. Natl. Acad. Sci. USA 98:10805*.
25. Murphy, K. M., A. B. Heimberger, and D. Y. Loh. 1990. Induction by antigen of intrathymic apoptosis of $CD4^+CD8^+$ TCR^{lo} thymocytes in vivo. *Science 250:1718*.
26. Haskins, K., R. Kubo, J. White, M. Pigeon, J. Kappler, and P. Marrack. 1983. The major histocompatibility complex-restricted antigen receptor on T-cells. I. Isolation with a monoclonal antibody. *J. Exp. Med. 157:1149*.
27. Lutz, M. B., N. Kukutsch, A. L. Ogilvie, S. Rossner, F. Koch, N. Romani, and G. Schuler. 1999. An advanced culture method for generating large quantities of highly pure dendritic cells from mouse bone marrow. *J. Immunol. Methods 223:77*.
28. Kamentsky, L. 2001. Laser scanning cytometry. *Methods Cell Biol. 63:51*.
29. Darzymkiewicz, Z., E. Bedner, X. Li, W. Gorczyca, and M. Melamed. 1999. Laser-scanning cytometry: a new instrumentation with many applications. *Exp. Cell Res. 249:1*.
30. Kubsch, S., E. Graulich, J. Knop, and K. Steinbrink. 2003. Suppressor activity of anergic T cells induced by IL-10-treated human dendritic cells: association with IL-2- and CTLA-4-dependent G_1 arrest of the cell cycle regulated by p27Kip1. *Eur. J. Immunol. 33:1988*.
31. Darzymkiewicz, Z., and E. Bedner. 2001. Use of flow and laser scanning cytometry to study mechanisms regulating cell cycle and controlling cell death. *Clin. Lab. Med. 21:857*.
32. Darzynkiewicz, Z., X. Li, and E. Bedner. 2001. Use of flow and laser scanning cytometry in analysis of cell death. *Methods Cell Biol. 66:69*.
33. Deptala, A., X. Li, E. Bedner, W. Cheng, F. Traganos, and Z. Darzymkiewicz. 1999. Differences in induction of p53, p21 WAF1 and apoptosis in relation to cell cycle phase of MCF-7 cells treated with camptothecin. *Int. J. Oncol. 15:861*.
34. Chen, D., V. Heath, A. O'Garra, J. Johnston, and M. McMahon. 1999. Sustained activation of the raf-MEK-ERK pathway elicits cytokine unresponsiveness in T cells. *J. Immunol. 163:5796*.
35. Boussiotis, V. A., G. J. Freeman, P. A. Taylor, A. Berezovskaya, I. Grass, B. R. Blazar, and L. M. Nadler. 2000. $p27^{kip1}$ functions as an anergy factor inhibiting interleukin 2 transcription and clonal expansion of alloreactive human and mouse helper T lymphocytes. *Nat. Med. 6:290*.
36. Jackson, S., A. Deloose, and K. Gilbert. 2001. Induction of anergy in Th1 cells associated with increased levels of cyclin-dependent kinase inhibitors $p21^{cip1}$ and $p27^{kip11}$. *J. Immunol. 166:952*.
37. Gauld, S. B., D. Blair, C. A. Moss, S. D. Reid, and M. M. Harnett. 2002. Differential roles for extracellularly regulated kinase-mitogen-activated protein kinase in B cell antigen receptor-induced apoptosis and CD40-mediated rescue of WEHI-231 immature B cells. *J. Immunol. 168:3855*.
38. Nel, A. E. 2002. T-cell activation through the antigen receptor. I. signaling components, signaling pathways, and signal integration at the T-cell antigen receptor synapse. *J. Allergy Clin. Immunol. 109:758*.
39. Nel, A. E., and N. Slaughter. 2002. T-cell activation through the antigen receptor. II. Role of signaling cascades in T-cell differentiation, anergy, immune senescence, and development of immunotherapy. *J. Allergy Clin. Immunol. 109:901*.
40. Maier, C. C., A. Bhandoola, W. Borden, K. Yui, K. Hayakawa, and M. I. Greene. 1998. Unique molecular surface features of in vivo tolerized T cells. *Proc. Natl. Acad. Sci. USA 95:4499*.
41. Fowler, S., and F. Powrie. 2002. CTLA-4 expression on antigen-specific cells but not IL-10 secretion is required for oral tolerance. *Eur. J. Immunol. 32:2997*.

42. Wells, A., M. Walsh, J. Bluestone, and L. Turka. 2001. Signalling through CD28 and CTLA-4 controls two distinct forms of T cell anergy. *J. Clin. Invest. 108:895*.
43. Schwartz, R. H. 2003. T cell anergy. *Annu. Rev. Immunol. 21:305*.
44. Appleman, L. J., A. Berezovskaya, I. Grass, and V. Boussiotis. 2000. CD28 costimulation mediates T cell expansion via IL-2-independent and IL-2-dependent regulation of cell cycle progression. *J. Immunol. 164:144*.
45. Colombetti, S., F. Benigni, V. Basso, and A. Mondino. 2002. Clonal anergy is maintained independently of T cell proliferation. *J. Immunol. 169:6178*.
46. Lee, I. H., W. P. Li, K. B. Hisert, and L. B. Ivashkiv. 1999. Inhibition of interleukin 2 signaling and signal transducer and activator of transcription (STAT)5 activation during T cell receptor-mediated feedback inhibition of T cell expansion. *J. Exp. Med. 190:1263*.
47. DeSilva, D. R., E. A. Jones, M. F. Favata, B. D. Jaffee, R. L. Magolda, J. M. Trzaskos, and P. A. Scherle. 1998. Inhibition of mitogen-activated protein kinase kinase blocks T cell proliferation but does not induce or prevent anergy. *J. Immunol. 160:4175*.
48. Davis, R. J. 1993. The mitogen-activated protein kinase signal transduction pathway. *J. Biol. Chem. 268:14553*.
49. Kaga, S., S. Ragg, K. A. Rogers, and A. Ochi. 1998. Stimulation of CD28 with B7-2 promotes focal adhesion-like cell contacts where Rho family small G proteins accumulate in T cells. *J. Immunol. 160:24*.
50. Delon, J., N. Bercovici, R. Liblau, and A. Trautmann. 1998. Imaging antigen recognition by naive $CD4^+$ T cells: compulsory cytoskeletal alterations for the triggering of an intracellular calcium response. *Eur. J. Immunol. 28:716*.
51. Valitutti, S., S. Muller, M. Salio, and A. Lanzavecchia. 1997. Degradation of T cell receptor (TCR)-CD3-ζ complexes after antigenic stimulation. *J. Exp. Med. 185:1859*.
52. Yu, H., D. Leitenberg, B. Li, and R. A. Flavell. 2001. Deficiency of small GTPase Rac2 affects T cell activation. *J. Exp. Med. 194:915*.
53. Sechi, A. S., J. Buer, J. Wehland, and M. Probst-Kepper. 2002. Changes in actin dynamics at the T-cell/APC interface: implications for T-cell anergy? *Immunol. Rev. 189:98*.